PERGAMON

Chaos, Solitons and Fractals 15 (2003) 233–244

CHAOS
SOLITONS & FRACTALS

www.elsevier.com/locate/chaos

Estimation of the dominant Lyapunov exponent of non-smooth systems on the basis of maps synchronization

Andrzej Stefański *, Tomasz Kapitaniak

Division of Dynamics, Technical University of Lodz, Stefanowskiego 1/15, 90-924 Lodz, Poland

Accepted 15 May 2002

Abstract

A novel method of estimation of the largest Lyapunov exponent for discrete maps is introduced and evaluated for chosen examples of maps described by difference equations or generated from non-smooth dynamical systems. The method exploits the phenomenon of full synchronization of two identical discrete maps when one of them is disturbed. The presented results show that this method can be successfully applied both for discrete dynamical systems described by known difference equations and for discrete maps reconstructed from actual time series. Applications of the method for mechanical systems with discontinuities and examples of classical maps are presented. The comparison between the results obtained by means of the known algorithms and novel method is discussed.

1. Introduction

The spectrum of Lyapunov exponents is the most precise tool for identification of the character of motion of a dynamical system and its estimation is one of the fundamental tasks in studies of these systems. These exponents are an exponential measure of divergence or convergence of nearby orbits in the phase space. From a mathematical point of view Lyapunov exponents are numbers describing the behaviour of the derivative of transformation along the phase trajectory. In practice, these exponents are a measure of sensitive dependence on initial conditions in phase space. For practical applications it is most important to know the largest Lyapunov exponent (LLE in further notation). If the largest value in the spectrum of Lyapunov exponents is positive it means that the system is chaotic. The largest value equal to zero indicates periodic system dynamics. If all Lyapunov exponents are negative, then the stable critical point is an attractor.

The idea of Lyapunov exponent was introduced by Oseledec [9]. His theoretical studies and numerical algorithms formulated by Benettin et al. [1,2] and Wolf et al. [14], allow an easy estimation of entire spectrum of Lyapunov exponents for smooth, continuous systems described by differential equation of motion and for discrete maps described by difference equations. If such equations are not known, or if the system under consideration is non-smooth, the estimation of Lyapunov exponents is not straightforward.

In recent years several methods for calculation of Lyapunov exponents for dynamical systems with discontinuities have been proposed. One of them is an application of the classical algorithm which is developed for cases of non-smooth systems [6]. The other one allows to determine LLE of the one-dimensional discrete map generated from the dynamical system under consideration [4,8]. There exist also the methods of estimation of the Lyapunov exponents which are based on the reconstruction of the attractor from time series [14] or chaos synchronization [11–13].

* Corresponding author.
E-mail address: steve@ck-sg.p.lodz.pl (A. Stefański).

0960-0779/03/$ - see front matter
PII: S0960-0779(02)00095-4

In this paper we describe a novel method of estimation of LLE for discrete dynamical systems using the phenomenon of ideal (full) [10] or practical [5] synchronization between two identical discrete maps—one disturbed and one undisturbed. The ideal synchronization takes place when all trajectories converge to the same value and remain in step with each other during further evolution (i.e. $\lim_{t\to\infty}|x(t)-y(t)|=0$ for two arbitrarily chosen trajectories $x(t)$ and $y(t)$). The practical synchronization is defined by the relation $\lim_{t\to\infty}|x(t)-y(t)|\leqslant\delta$ where δ is a vector of small parameters.

The presented approach is based on the authors' [11–13] and other researchers' [3] theoretical studies. These considerations show, that two identical dynamical systems coupled by unidirectional negative feedback mechanisms—as it is given by the equations:

$$\begin{aligned}\dot{x}&=f(x),\\ \dot{y}&=f(y)+d(x-y),\end{aligned}\tag{1}$$

(where $x,\ y\in\mathbf{R}^n$ and $d\in\mathbf{R}^n$ is a coupling coefficient) can synchronize if the coupling coefficient is larger than LLE ($\lambda_{\max}$) which characterizes the coupled systems ($d>\lambda_{\max}$). This linear dependence between the rate of coupling and Lyapunov exponents results from the linearized solution of Eq. (1), describing the time evolution of a distance $z(t)=x(t)-y(t)$ between the trajectories representing both coupled systems, for small value of $z(t)$. Such a solution (starting from $z(0)$) has a following form:

$$z(t)=z(0)\exp[(\lambda_{\max}-d)t].\tag{2}$$

It is obvious, that the effect given by Eq. (2) cannot appear for a pair of discrete maps coupled in a way given by Eq. (1). However, the similar synchronization effect for two identical maps can be achieved by the disturbance of one map. This disturbance is under control of another map dynamics and appropriate exponential function. The properties of such synchronization have been exploited to work out the presented method.

Our results show that this approach can be successfully applied both for discrete dynamical systems described by known difference equations and for discrete maps reconstructed from actual time series. Since the synchronization is easily detectable, the method has significant practical advantage over more traditional algorithmic methods in dealing with non-smooth systems.

2. Theoretical studies

Consider a pair of discrete dynamical systems given by two identical maps

$$\begin{aligned}x_{n+1}&=f(x_n),\\ y_{n+1}&=f(y_n),\end{aligned}\tag{3}$$

where $x,y\in\mathbf{R}$, evolving on the asymptotically stable chaotic attractor $\boldsymbol{A}$. In such a case the evolution on the attractor $\boldsymbol{A}$ is characterized by one positive Lyapunov exponent. The sequences of iterations generated from Eq. (3) starting from different initial conditions ($x_0\neq y_0$) represent two independent trajectories on the attractor $\boldsymbol{A}$.

Let us introduce a new variable z representing the distance between the trajectories of the systems under consideration after each iteration, given by

$$z=x-y,\tag{4}$$

where $z\in\mathbf{R}$. It follows that the evolution of variable z is determined by the difference equation

$$z_{n+1}=x_{n+1}-y_{n+1}=f(x_n)-f(y_n).\tag{5}$$

For small values of z, i.e. $z\ll|\boldsymbol{A}|$, where $|\boldsymbol{A}|\in\mathbf{R}\geqslant 0$ is the attractor size (maximum distance between two points on the attractor), we can assume that the distance between trajectories of the systems under consideration after n iterations is given by the linearized equation resulting from the definition of Lyapunov exponent, viz

$$z_n=z_0\exp(\lambda n),\tag{6}$$

where λ is a Lyapunov exponent and z_0 is initial distance between the trajectories. According to Eq. (6) the difference equation of the trajectory separation is

$$z_{n+1}=z_n\exp(\lambda).\tag{7}$$

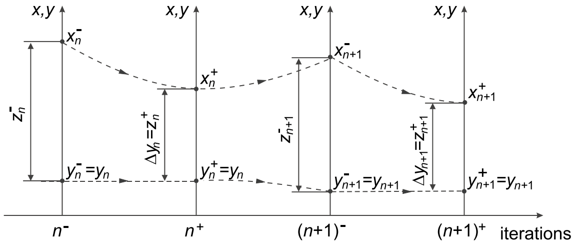

Fig. 1. The scheme of disturbance mechanisms.

In other words, for nearby trajectories the separation increases (positive value of λ) or decreases (negative value of λ) at a rate proportional to Lyapunov exponent.

Let us now perturb the value of x_n at each step according to a mechanism described below. The scheme of this mechanism is shown in Fig. 1.

A new value of x_n at each step is $y_n + \Delta y_n$, i.e. let

$$x_n^- \to x_n^+ = y_n + \Delta y_n, \tag{8}$$

where the indices "−" and "+" refer to values of x_n before and after perturbation. If Δy_n were equal to z_n^-, there would be no perturbation, instead we impose perturbation by allotting to $\Delta y_n \in \mathbf{R}$ disturbance value

$$\Delta y_n = z_n^- \exp(-p), \tag{9}$$

where $p \in \mathbf{R}$ is a convergence parameter.

Then the disturbance value evolves according to

$$\Delta y_{n+1}/\Delta y_n = \left(z_{n+1}^-/z_n^+\right)\exp(-p). \tag{10}$$

Next substituting Eq. (8) in Eq. (3), we obtain

$$x_{n+1} = f(y_n + \Delta y_n), \tag{11a}$$

$$y_{n+1} = f(y_n). \tag{11b}$$

Written in this form, we can regard Eq. (11a) as the disturbed version of the undisturbed trajectory represented by Eq. (11b). However, if the separation of these trajectories is small, the Lyapunov exponent expression given by Eq. (7) is also valid. Moreover, substituting Eqs. (11a) and (11b) in Eq. (10) gives

$$\Delta y_{n+1} = [f(y_n + \Delta y_n) - f(y_n)]\exp(-p), \tag{12}$$

since

$$z_n^+ = x_n^+ - y_n = \Delta y_n. \tag{13}$$

It is clear from Eqs. (9) and (10) that full synchronization of the disturbed and undisturbed maps occurs when the *disturbance* achieves zero value.

Using Eqs. (13) and (10), we can describe the evolution of the disturbance value in the following form

$$\Delta y_{n+1} = \Delta y_n \exp(\lambda - p). \tag{14}$$

It is clear from Eq. (12) that fulfilling the inequality

$$p > \lambda \tag{15}$$

guarantees the decrease of the disturbance value to zero and causes the synchronization of disturbed and undisturbed systems (Eqs. (11a) and (11b)). In such a case the synchronization manifold $x = y$ becomes an attractor, i.e. the evolution of the two-dimensional system defined by Eqs. (11a) and (11b) is reduced to the evolution on the one-dimensional attractor $\boldsymbol{A}$ located on the $x = y$ manifold. In the opposite case ($p < \lambda$) the manifold $x = y$ is a repeller, and synchronization is impossible.

Moreover, from Eq. (12) we see that the disturbance value is the product of two independent factors:

(1) exponential divergence or convergence of nearby trajectories with a rate proportional to positive or negative Lyapunov exponent,
(2) exponential divergence or convergence (it depends on the sign of parameter p) due to the introduced disturbance with a rate proportional to the parameter p.

The first factor is a valid representation only in a direct neighbourhood of the synchronized state (small Δy value) where linear effects are dominant. The second one acts in the entire phase space. Thus the product of exponential effects is valid only near the synchronized manifold $x = y$. From Eq. (12) also results that one of them counteracts the other (for the same signs of λ and p).

Let us now consider a k-dimensional discrete system. Using the substitutions $y_i' = y(i)_{n+1}$ and $y_i = y(i)_n$ we can describe such a system in the following form

$$y_i' = f(y_i), \tag{16}$$

where $y \in \mathbf{R}^k$, $i \in (1, 2, \ldots, k)$. Substituting Eq. (16) in Eqs. (11a), (11b) and (12) an augmented system is as follows

$$x_i' = f(y_i + \Delta y_i), \tag{17a}$$

$$y_i' = f(y_i), \tag{17b}$$

$$\Delta y_i' = [f(y_i + \Delta y_i) - f(y_i)] \exp(-p), \tag{17c}$$

where $x, y, \Delta y \in \mathbf{R}^k$. The evolution of the k-dimensional discrete map is described by k Lyapunov exponents. Hence, the synchronization between disturbed and undisturbed maps (Eqs. (11a) and (11b)) is guaranteed by the inequality

$$p > \lambda_{\max}, \tag{18}$$

where $\lambda_{\max}$ is LLE of the system under consideration (Eq. (16)).

Comparing Eqs. (14) and (2), it is clearly visible, that the assumed exponential nature of the disturbance (Eq. (7)) is not casual because such form of perturbation leads to the same linear dependence between LLE and the convergence parameter p as between this exponent and coupling coefficient for coupled continuous systems. Hence, this dependence can also be used for an estimation of LLE of discrete maps.

3. Numerical estimation procedure

Eq. (18) allows us to propose a novel method of estimation of LLE for k-dimensional discrete dynamical systems. In fact Eq. (18) states that the smallest value of the coefficient p for which synchronization takes place is equal to the maximum Lyapunov exponent $\lambda_{\max}$.

To apply our method for any discrete dynamical system (Eq. (16)) it is necessary to build an augmented system according to Eqs. (17a)–(17c) or to formulate a numerical process which fulfils Eqs. (17a)–(17c) in several steps. The next action is numerical search for the smallest synchronization parameter p for a such system, which approximates to LLE of the investigated system (Eq. (16)).

The simplest way to find the smallest synchronization value of coefficient p is to construct a bifurcation diagram of the *disturbance* value Δy against the parameter p. Examples of such diagrams are presented in Fig. 2 for the Henon map

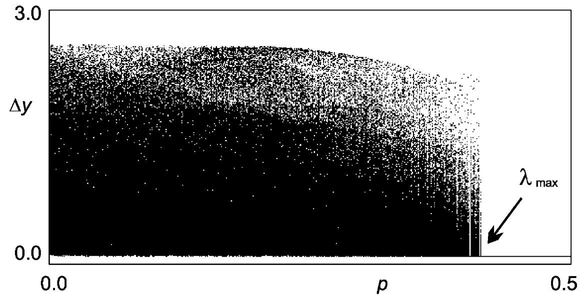

Fig. 2. Bifurcation diagram of the disturbance value Δy against the parameter p for the system given by Eq. (20) (Henon map): $a = 1.40$, $b = 0.30$.

(Eq. (20)) applied in Eqs. (17a)–(17c). We can obtain the searched value of p from the point on the horizontal p-axis where disturbance Δy achieves zero value. However, using such a way for LLE estimation is time consuming.

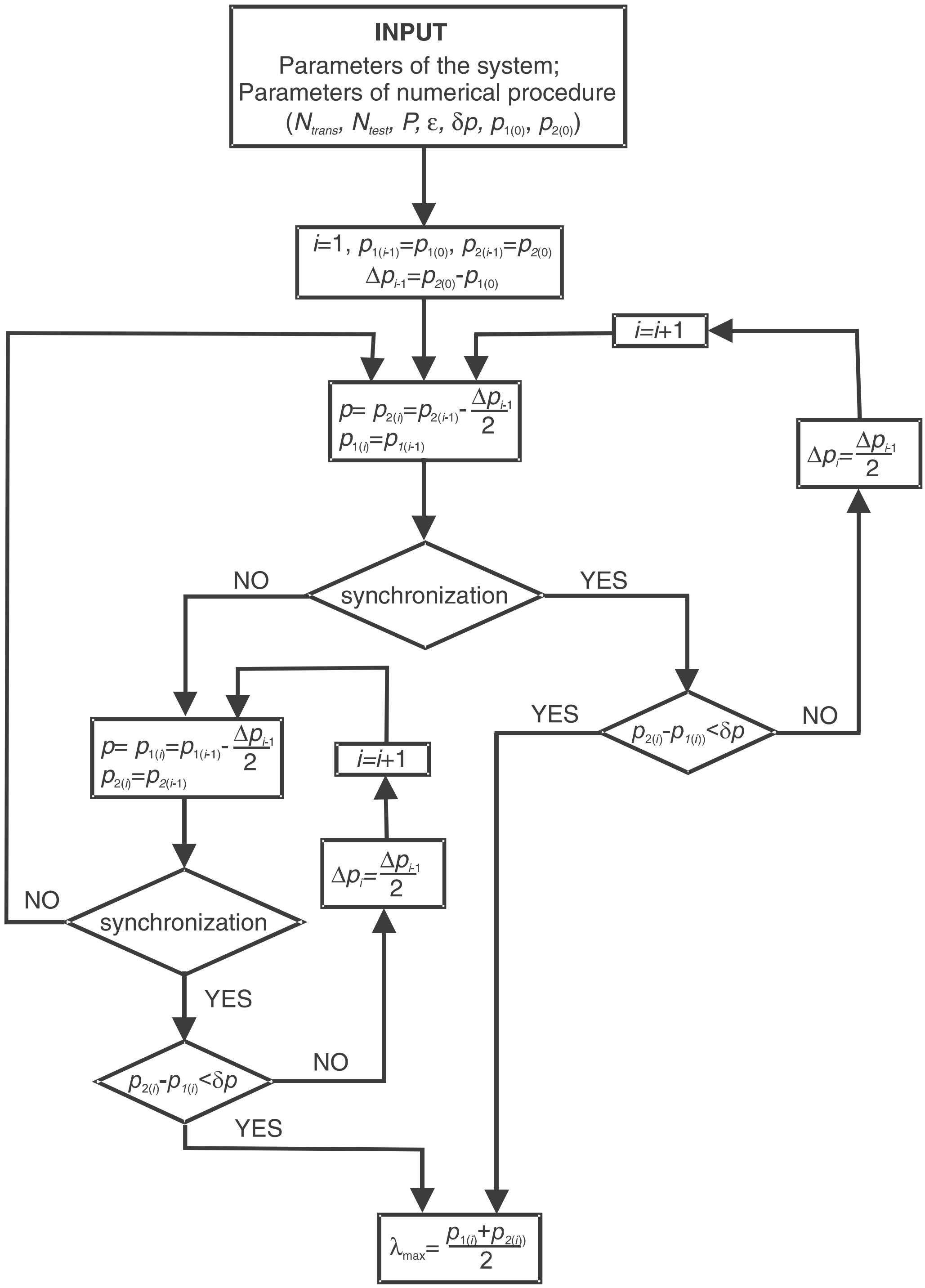

Fig. 3. The scheme of the numerical investigation procedure of the LLE.

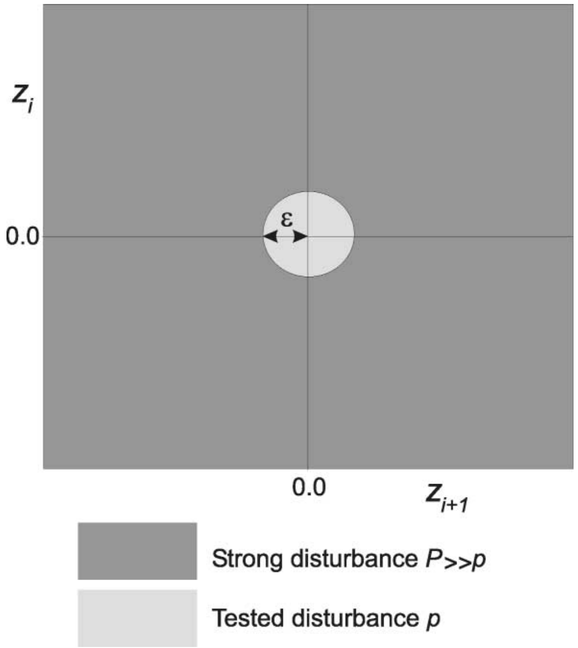

Fig. 4. The idea of *elastic disturbance parameter.*

Therefore, for most of the calculations presented in this paper, we have applied a method of fast search of the synchronization p value in tentatively assumed range of the convergence parameter—$\Delta p_0 = p_{1(0)} - p_{2(0)}$. This method consist in division in half of the Δp_i range depending on an occurrence of synchronization ($p_i = p_{2(i-1)} - \Delta p_{i-1}/2$) or desynchronization ($p_i = p_{1(i-1)} + \Delta p_{i-1}/2$) until the range Δp_i is less than assumed precision of estimation δp. A scheme of this procedure is shown in Fig. 3.

A long time of transient motion before both investigated maps achieve the synchronized state is a disadvantage which can occur during the numerical analysis. In particular, this effect appears for small negative difference between LLE and convergence parameter ($\lambda_{\max} - p \approx 0$). To eliminate this disadvantageous effect and to achieve synchronization faster, we have assumed two different values of the parameter p depending on the distance between the investigated trajectories (see Fig. 4). The first of them is the current tested value of the parameter p which is valid only in a direct neighbourhood of the synchronization manifold $z = 0$. This region is limited by a boundary value ε (in light grey in Fig. 4). Beyond this region, the convergence parameter becomes much larger than its tested value ($P \gg p$, in dark grey in Fig. 4). It forces the second system (disturbed) to evolve in the neighbourhood of the undisturbed system and it accelerates the process of the appearance of synchronization.

The second way to shorten the estimation procedure is to detect of the practical synchronization because it is enough to confirm that the synchronization state is asymptotically stable for the investigated value of the parameter p. For this purpose, the assumed constant number of iterations N (for each tested value of convergence parameter) is divided into two parts: transient iterations N_{trans} and tested N_{test} iterations ($N = N_{\text{trans}} + N_{\text{test}}$). On the basis of the numerical analysis, we can assume that the synchronized state is stable if the distance between the trajectories does not cross the boundary value ε during the tested iterations i.e. the practical synchronization takes place.

4. Applications of the method

In this section we present the examples of our method applied in two cases:

(i) for a discrete map of a known difference equation,
(ii) for a discrete map obtained from a dynamical system with discontinuities.

4.1. Discrete map of known difference equation

As an example we have used the classical Henon ($k = 2$) map which after the substitution in Eq. (16) is described by the following difference equations:

$$y'_1 = 1 - ay_1^2 + y_2,\qquad y'_2 = by_1, \tag{19}$$

where a, b are parameters.

After putting Eq. (19) into Eqs. (17a)–(17c) the augmented system takes the forms

$$\begin{aligned} x'_1 &= 1 - a(y_1 + \Delta y_1)^2 + (y_2 + \Delta y_2),\\ x'_2 &= b(y_1 + \Delta y_1),\\ y'_1 &= 1 - ay_1^2 + y_2,\\ y'_2 &= by_1,\\ \Delta y'_1 &= [\Delta y_2 - a\Delta y_1(\Delta y_1 + 2y_1)]\exp(-p),\\ \Delta y'_2 &= b\Delta y_1 \exp(-p). \end{aligned} \tag{20}$$

In Fig. 5 we show: a bifurcation diagram (Fig. 5a) of the Henon map (Eq. (19)) and corresponding LLE obtained using a classical algorithm (Fig. 5b) and our method (Fig. 5c). More detailed comparison between the values of LLEs (for chosen values of system parameters) is shown in Table 1. The calculations of LLEs presented in Fig. 5b and column II in Table 1 have been carried out by means of software DYNAMICS [7]. Comparing both the values in Table 1 and

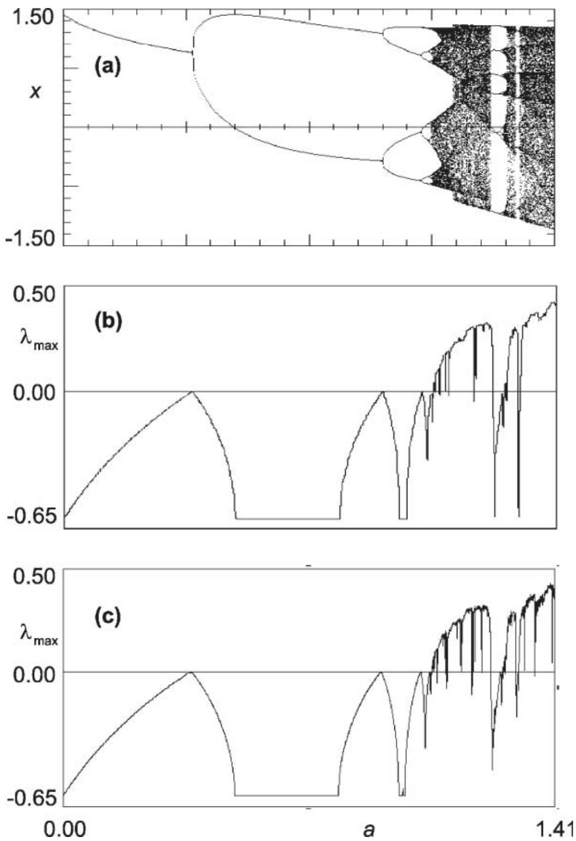

Fig. 5. Bifurcation diagram of Henon map (a) and corresponding Lyapunov exponents: obtained by means of classical algorithm (b), obtained by means of novel method (c): $b = 0.3$. Parameters of the numerical procedure: $p_{1(0)} = -0.8$, $p_{2(0)} = 0.8$, $\varepsilon = 0.005$, $\delta p = 0.001$, $P = 1.00$.

Table 1
The comparison of LLEs of Henon map

(I) Parameters	(II) Classical algorithm (λ_{max})	(III) Novel method (λ_{max})
$a = 1.40$, $b = 0.30$	0.4186	0.4050
$a = 1.10$, $b = 0.30$	0.1811	0.1830
$a = 0.70$, $b = 0.30$	−0.6019	−0.6020
$a = 0.30$, $b = 0.30$	−0.0785	−0.0770

diagrams in Fig. 5b and c we can see, that for the maps of the known difference equation, our method approximates the classically calculated results with good precision.

4.2. Discrete maps of a linear oscillator with impacts

In this example we apply our method to estimate LLE of a discrete impact and Poincare maps generated from the dynamics of a linear impact oscillator. The differential equations describing such an oscillator can be written as follows:

$$\begin{aligned} x_1 < X_0: \quad & \dot{x}_1 = x_2, \\ & \dot{x}_2 = q\cos(\eta t) - \alpha^2 x_1 - 2hx_2, \\ x_1 \geqslant X_0: \quad & x_{2a} = -Rx_{2b}. \end{aligned} \tag{21}$$

In the above equations parameter α represents natural frequency, h—linear damping, q—amplitude of excitation, η—frequency of forcing, X_0 is a position of the buffer, R is coefficient of restitution, x_{2b} is the velocity in a moment before the impact and x_{2a} is the velocity just after the impact. The examples of the impact and Poincare maps of the system given by Eq. (21) and corresponding phase portrait, for chosen values of parameters, are shown in Fig. 6. The difference equations describing these maps can be written in the following general form:

$$\begin{aligned} \upsilon_{n+1} &= f(\upsilon_n, \xi_n), \\ \xi_{n+1} &= g(\upsilon_n, \xi_n), \end{aligned} \tag{22}$$

where υ and ξ represent the velocity v and the phase of excitation force θ at the moment of the impact in impact map (Fig. 6c) or the velocity u and the position x after each period of excitation in a Poincare map (Fig. 6b). Expressions defining the right sides of Eq. (22) are not known. Forms of transition from previous to the next iteration are reconstructed numerically from differential equations describing the investigated system (Eq. (21)). Hence, the impact map Σ_I and Poincare map Σ_P can be defined as follows:

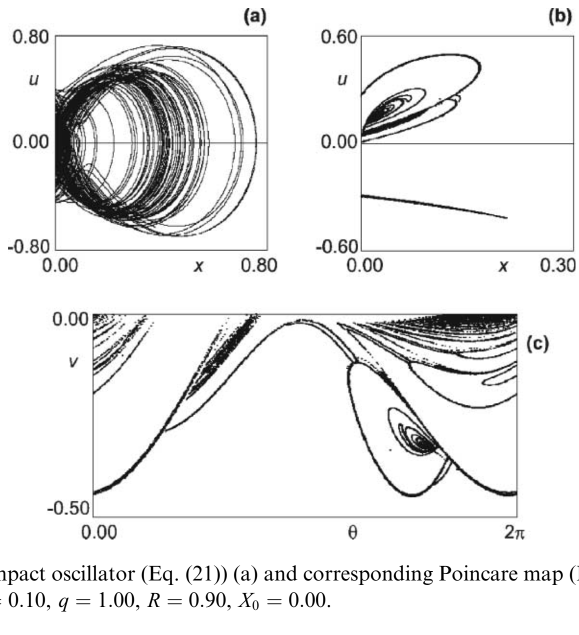

Fig. 6. The phase portrait of the impact oscillator (Eq. (21)) (a) and corresponding Poincare map (Eq. (23a)) (b) and impact map (Eq. (23b)) (c): $\eta = 3.150$, $\alpha = 1.00$, $h = 0.10$, $q = 1.00$, $R = 0.90$, $X_0 = 0.00$.

$$\Sigma_I = \begin{cases} v_n = v(t) \to v_{n+1} = v(t+\tau_n), \\ \theta_n = \cos^{-1}(\eta t) \to \theta_{n+1} = \cos^{-1}(\eta(t+\tau_n)), \end{cases} \tag{23a}$$

$$\Sigma_P = \begin{cases} x_n = x(t) \to x_{n+1} = x(t+2\pi/\eta), \\ u_n = u(t) \to u_{n+1} = u(t+2\pi/\eta), \end{cases} \tag{23b}$$

where τ_n—time between the impacts in given iteration n.

Substituting Eq. (22) in Eq. (15) we obtain the augmented system in the form appropriate to apply the estimation procedure

$$\begin{aligned} \upsilon_1' &= f(\upsilon_2 + \Delta\upsilon, \xi_2 + \Delta\xi), \\ \xi_1' &= g(\upsilon_2 + \Delta\upsilon, \xi_2 + \Delta\xi), \\ \upsilon_2' &= f(\upsilon_2, \xi_2), \\ \xi_2' &= g(\upsilon_2, \xi_2), \end{aligned} \quad \to \quad \begin{aligned} \Delta\upsilon' &= (\upsilon_1' - \upsilon_2')\exp(-p), \\ \Delta\xi' &= (\xi_1' - \xi_2')\exp(-p). \end{aligned} \tag{24}$$

The transition to the next iteration is divided into two steps for the sake of unknown functions of transition.

The results of the carried out estimation of the dominant Lyapunov exponent using the proposed method are presented in Fig. 7 and Table 2. In Fig. 7 we show the bifurcation diagram (Fig. 7a) of the impact oscillator (Eq. (21)) and the diagrams presenting corresponding LLEs estimated on the basis of impact maps synchronization (Fig. 7b) and Poincare maps synchronization (Fig. 7c). We can see the bands when chaotic motion occurs (see Fig. 7a) when Lyapunov exponent takes positive value (Fig. 7b and c). Also periodic motion occurs when negative Lyapunov exponent is found in these figures.

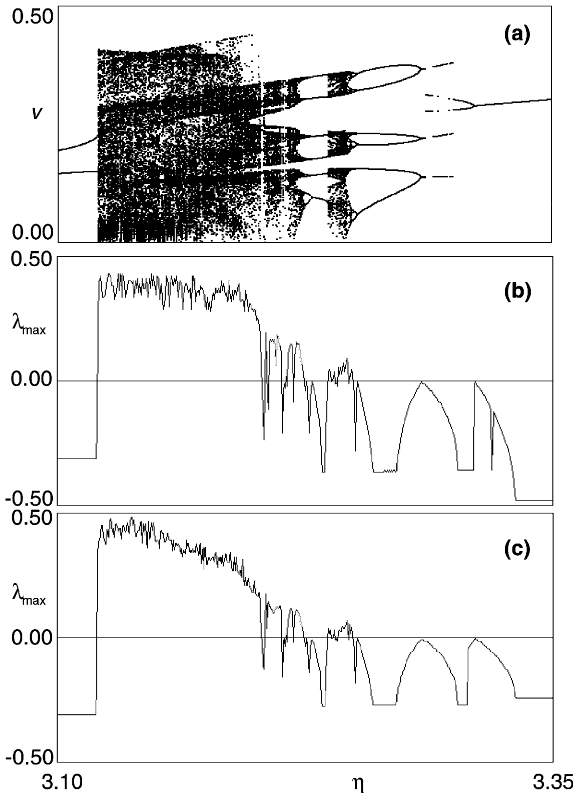

Fig. 7. Bifurcation diagram of the impact oscillator (Eq. (21)) presenting velocity in moment after impact versus bifurcation coefficient η (a) and corresponding Lyapunov exponents: obtained from impact map (λ_I) (b), obtained from Poincare map (λ_P) (c). Parameters of the impact oscillator: $\alpha = 1.00$, $h = 0.10$, $q = 1.00$, $R = 0.90$, $X_0 = 0.00$. Parameters of the numerical procedure: $N_{\text{trans}} = 800$, $N_{\text{test}} = 700$, $p_{1(0)} = -0.7$, $p_{2(0)} = 0.7$, $\varepsilon = 0.01$, $\delta p = 0.01$, $P = 1.00$.

Table 2
The comparison of LLEs of the considered system (Eq. (21)): $\alpha = 1.00$, $h = 0.00$, $q = 1.00$, $R = 0.80$, $X_0 = 0.00$

(I) η	(II) T/τ_A	(III) r_A	(IV) D-maps λ_D	(V) Impact maps		(VI) Poincare maps	
				(Va) λ_I	(Vb) $\lambda_D + \ln(r_A)$	(VIa) λ_P	(VIb) $(\lambda_D T/\tau_A)$
3.00	1.000	0.992	−0.2230	−0.2230	−0.2310	−0.2240	−0.2230
3.105	1.182	0.986	0.2038	0.1890	0.1897	0.2380	0.2410
3.121	1.250	0.993	−0.2230	−0.2230	−0.2302	−0.2790	−0.2780
3.126	1.065	0.988	0.2015	0.1930	0.1892	0.2270	0.2145

In Table 2 the values of LLE (for chosen values of the system (Eq. (21)) parameters) achieved using our method and calculated by means of other known algorithm which can be applied for discontinuous systems are shown. These parameters are the same as those used by other authors [4,8], in order to simplify the comparison of the results.

5. Discussion and conclusions

The numerical examples presented in the previous section show, that in case the of a known difference equation describing the map under consideration, the proposed method approximates the classically calculated results satisfactorily. The difference between the values of Lyapunov exponent in both cases does not cross a threshold of several percent.

However, the comparison of the results obtained for an impact oscillator (Table 2) requires more detailed analysis of the differences between these results and their reasons. The values of LLE (λ_H) presented in the second column of Table 2 have been determined on the basis of the other method for discrete map generated from the analyzed system (Eq. (21)) [4,8]. The construction of such a map causes, that a dependence between Lyapunov exponents achieved from this map (D-map) and calculated using other known methods [6], for the systems (phase streams) with discontinuities, is given as follows

$$\lambda_D = \lambda_{de}\tau_A, \tag{25}$$

where λ_D and λ_{de} are LLEs determined appropriately from the D-map and differential equations (Eq. (21)) and τ_A is an average time between the impacts.

During the estimation of LLEs from impact maps (Eq. (23a)) there appears an additional convergential effect connected with the coefficient of restitution R. In the moment of impact, the trajectory separation z changes in each iteration i according to the transformation

$$z(i)_b = \sqrt{(\Delta v(i)_b)^2 + (\Delta\theta(i)_b)^2} \rightarrow z(i)_a = \sqrt{(R\Delta v(i)_b)^2 + (\Delta\theta(i)_b)^2}. \tag{26}$$

The indices "b" and "a" refer to the states before and after the impact. Hence, the relation between LLEs for impact and H-maps takes the form:

$$\lambda_I = \lambda_D + \ln(r_A), \tag{27}$$

where

$$r_A = \frac{1}{n}\sum_{i=1}^{n}(z(i)_a/z(i)_b) \tag{28}$$

is an average relative decrease of the trajectory separation after impact (column III in Table 2).

According to Eq. (27) LLEs generated from impact maps are smaller than these obtained form D-maps, because $\ln(r)$ has a negative value ($r < 1$ in column III in Table 2). It is confirmed by comparison of estimated LLEs with the values calculated from Eq. (28) (columns Va and Vb in Table 2), but only for positive LLEs.

It is clear, that the connection between LLEs determined from differential equations of smooth system and these estimated from its Poincare map is given by equality

$$\lambda_P = \lambda_{de}T, \tag{29}$$

where $T = 2\pi/\eta$—period of excitation.

In the case of non-smooth systems this relation (Eq. (29)) can assume more complicated form due to the effect of convergence caused by an impact, similar to that, described by Eqs. (26) and (28) for an impact map. However, the results presented in Table 2 (columns VIa and VIb) show that Eq. (30) works well enough also in the system under consideration and the dependence between *D*-map and Poincare map methods is given by

$$\lambda_P \approx (T/\tau_{\mathrm{A}})\lambda_D. \tag{30}$$

The comparative analysis presented in Table 2 shows that the convergence effect of the impact described above (Eq. (28)) influences positive values of LLEs only, especially when proposed method is applied for impact maps. For negative Lyapunov exponents almost ideal agreement of the results, obtained by means of novel and known method, is observed (columns IV, Va, VIb). This phenomenon can be explained easily. Namely, the effect of the largest positive or negative Lyapunov exponent (for nearby trajectories) takes place only in temporary direction connected with this exponent, because the spatial orientation of the directions connected with given exponent varies in very complicated way during the evolution on the attractor. The convergence due to the impact also acts only in a given direction of the map. Since the disturbance effect, associated with exponent p, acts in all directions of the map with the same rate, so for the chaotic impact map the convergence caused by positive value of p is strengthened by impact convergence in each iteration and synchronization is possible for parameter p smaller than LLEs according to Eq. (27). However, in the case of periodic maps the negative LLE effect is covered by the impact effect only accidentally in some iterations due to the disagreement of main directions of these both effects in most iterations. Therefore, the strengthening of the convergence is not effective, so the synchronization appears only when condition given by Eq. (18) is fulfilled.

In fact, the above described small differences between LLEs estimated from our procedure and obtained from other algorithm have no practical significance for the proper identification of motion character. In Figs. 6 and 7 we show that the proposed method is a good enough tool for the detection of deterministic chaos and bifurcation values of parameters.

Summing up, we can state that the method we have demonstrated allows us to estimate the value of LLEs both for discrete dynamical systems of known difference equations and also for discrete maps reconstructed from the time evolution of the given system. The novelty of the method lies in its use of the phenomenon of synchronization (readily recognized) of two identical discrete maps, one disturbed by the other. The approach presented in this paper can be generalized to higher dimensional systems. From a viewpoint of practical applications, the presented method can be very useful for the estimation of the LLE in mechanical systems with discontinuities, in particular for systems with impacts or dry friction, where classical methods are not easily applicable.

Acknowledgements

This work has been supported by Polish Committee for Scientific Research (KBN) under the project no. 7 T07A 005 19.

References

[1] Benettin G, Galgani L, Giorgilli A, Strelcyn JM. Lyapunov exponents for smooth dynamical systems and Hamiltonian systems; a method for computing all of them, Part I: Theory. Meccanica 1980;15:9–20.
[2] Benettin G, Galgani L, Giorgilli A, Strelcyn JM. Lyapunov exponents for smooth dynamical systems and Hamiltonian systems; a method for computing all of them, Part II: Numerical application. Meccanica 1980;15:21–30.
[3] Fujisaka H, Yamada T. Stability theory of synchronized motion in coupled-oscillator systems. Progress Theor Phys 1983;69(1):32–47.
[4] Hinrichs N, Oestreich M, Popp K. Dynamics of oscillators with impact and friction. Chaos, Solitons & Fractals 1997;4(8):535–58.
[5] Kapitaniak T, Sekieta M, Ogorzalek M. Monotone synchronization of chaos. Bifurcation Chaos 1996;6:211–5.
[6] Müller P. Calculation of lyapunov exponents for dynamical systems with discontinuities. Chaos, Solitons & Fractals 1995;5(9):1671–81.
[7] Nusse HE, Yorke JA. Dynamics: numerical explorations. New York: Springer-Verlag; 1997.
[8] Oestreich M. Untersuchung von schwingern mit nichtglatten kennlinien. Düsseldorf: VDI Verlag GmbH; 1998.
[9] Oseledec VI. A multiplicative ergodic theorem: Lyapunov characteristic numbers for dynamical systems. Trans Moscow Math Soc 1968;19:197–231.
[10] Pecora LM, Carroll TL. Synchronization of chaos. Phys Rev Lett 1990;64:221–4.
[11] Stefański A, Kapitaniak T. Using chaos synchronization to estimate the largest Lyapunov exponent of non-smooth systems. Discrete Dyn Nature Soc 2000;4:207–15.

[12] Stefański A. Estimation of the largest Lyapunov exponent in systems with impacts. Chaos, Solitons & Fractals 2000;11(15):2443–51.

[13] Stefański A, Kapitaniak T, Brindley J. A simple method of chaos detection in mechanical systems with discontinuities. ASME Design Engineering Technical Conferences, Pittsburgh, USA, 2001 (on CD-ROM).

[14] Wolf A, Swift JB, Swinney HL, Vastano JA. Determining Lyapunov exponents from a time series. Physica D 1985;16:285–317.